Spectral and Electrochemical Sensing Studies of Novel Tetradentate Schiff Bases, Having Enhanced Antifungal Activity, Containing Ferrocene and Aromatic Moieties Attached Imines

Dhasarathan Saranya, Shunmugaperumal Selvaraj, Ponnurangam Kamatchi Selvaraj*[+]

PG & Research Department of Chemistry, Government Arts College for Men (Autonomous), Nandanam, Chennai-600 035, Tamil Nadu, INDIA

ABSTRACT: *Multi metal ion sensing unsymmetrical Schiff bases containing ferrocene group attached imine at one side and aromatic moiety connected azomethine on the other side have been synthesized. Titration studies coupled with a UV-Visible spectrophotometer expose the binding aptitude of new receptors. Development of MLCT band near 457 nm for the coordination of Cu^{2+} ions with new ligands is also noticed. Electrochemical studies of receptor solutions with added metal ions expose quasi-reversible processes by giving superfluous ΔE_P values (146-161 mV, then the expected 59 mV). The concentration of metal ions required for effective sensing is calculated from the percentage amount of ΔI_{pa} extracted from the I_{pa} data. Results obtained in computational molecular docking studies and in-vitro analysis invite more focused research by the pharmacist to develop new formulations for antifungal medicines.*

KEYWORDS: *Antifungal Compound; Binding Attitude; Cation Sensors; In-vitro; Molecular Docking.*

INTRODUCTION

Scientists in the field of Material science, Chemistry, Physics, and Biology looking for small abiotic molecules capable of binding discriminatively (reversibly or irreversibly) to different metal ions with a simultaneous noticeable change in the potential value of oxidation state or modification in the absorption and emission spectra of the employed component [1]. Chemosensors are tiny molecules that find application in different fields including clinical areas [2-5] for the reason that diminutive toxins and heavy metal ions cause health and environmental deterioration. Effluent from various industries, volcanic explosion and farming activities introduce cations and anions which affect the environment as well as the health of humans [6] Low sensitivity and longer time duration are associated with instrumentation techniques utilized to identify hazardous metal ions [7]. Chemosensors primed from Schiff base reactions in the form of ligands and metal complexes have a wide range of applications in many fields including systematic analysis, biochemical investigations, and antimicrobial studies [8-10].

Mercury ions, the greatest toxic heavy and transition metal ions, found in the aquatic system can root impairment

***** *To whom correspondence should be addressed.*
+ *E-mail: porbal96@gmail.com*
1021-9986/2022/9/2946-2960 *9/$/5.09*

to the kidney, central nervous system, offspring of a mammal, and toddlers [11]. Though copper ions are involved in many metabolic activities of humans [12], unfettered intake of copper ions may lead to degeneration of the nervous system [13] and detriment to the liver & kidney [14]. Alternation in the function of proteins present in enzymes having metal ions like zinc and ferrous resulted from the ingestion of nickel ions [15]. Manganese ions toxicity comprises vacillation in brain function, low appetite, crippling of neural function, and vehement activity [16]. Protein metallothionein transmits Cd^{2+} ions to the kidney. The extended biotic half-life period of Cd^{2+} ions gives amassed toxic effects and affects the kidney and develops prostate cancer [17]. Accumulation of Pb^{2+} ions in blood diminishes hearing ability in children and postponements adolescents' sexual maturity [18].

An enormous amount of ligands and their transition metal ion coupled complexes have been synthesized and used as models to mimic the biological activities of enzymes [19]. Not only that, Schiff bases are used in diverged fields including analytical, pharmaceutical, medical, and environmental research field [20].

Herein, the synthesis of new synthetic unsymmetrical Schiff bases *N*'1-((*E*)-2-(nitro)benzylidene)-*N*'4-((*E*)-2-(ferrocenylidene)succinohydrazide and *N*'1-((*E*)-2-hydroxy-5-(nitro)benzylidene)-*N*'4-((*E*)-2-(ferrocenylidene)succinohydrazide possessing ferrocene component at one end and aromatic group at another end of the foremost structure is reported. The presence of azomethine (-CH=N) groups with lone pair of electrons on sp^2 hybridized nitrogen atom is responsible for antifungal, antibacterial, and anticancer activities of Schiff base ligands and complexes [21]. Revelation of enhanced antifungal bustle rather than antibacterial activity of the newly prepared receptors alarms more pharmaceutical research to be carried out to bridge the gap between available antibacterial and antifungal commixture [22].

EXPERIMENTAL SECTION

Materials

Succinic anhydride, hydrazinehydrate, ferrocenecarboxaldehyde, 2-hydroxy-5-nitrobenzaldehyde, 2-nitrobenzaldehyde, and silica gel (Analytical grade) were purchased from E. Merck industry and used without further purification. Analytical grade $HgCl_2$, $Pb(OAc)_2$, $NiCl_2$, $Cd(OAc)_2$, $CuCl_2$ and $MnCl_2$, used in the cyclic voltammetry and UV-Visible titration studies were procured from Sigma–Aldrich. HPLC grade acetonitrile acquired from E- Merck and spectral grade absolute ethanol secured from Commercial Alcohols, Canada was used for spectral studies. Pure tetrabutylammoniumperchlorate [99+%] obtained from Chemical Center, Mumbai was used as such without purification.

Instruments

Mass spectra were documented in Bruker Daltonics esquire 3000 spectrometers. Proton NMR spectra were taken in BRUKER AVANCE spectrometer [500 MHz] engaging C_2D_5OD solvent. Using KBr pellets, FTIR spectra in the range of 400-4000 cm^{-1} were recorded in Perkin-Elmer 337 spectrometer. SHIMADZU MODEL UV-1800 240 V spectrophotometer was tied up to register UV–visible spectral studies between 200 and 800 nm. Electrochemical analyzer 1200B model having glassy carbon as the working electrode, Ag/AgCl as the reference electrode, and platinum as the counter electrode was employed to register cyclic voltammograms. TBAP solution (handled under care) was used as a supporting electrolyte. Elements like C, H, and N were analyzed with Herarus C-H-N rapid analyzer.

Synthesis of N'1-((E)-2-(nitro)benzylidene)-N'4-((E)-2-(ferrocenylidene)succinohydrazide [R1]

A modified procedure reported in the literature [23] was used to prepare the precursor compound succinic acid dihydrazide. To a solution of succinic anhydride (0.05 moles in 50 mL of ethanol) another solution containing hydrazine hydrate (0.12 moles) in 150 mL of ethanol was added in drops along with stirring and then the mixture was refluxed for 24 hours. Precipitated succinic acid dihydrazide was dried and recrystallized from ethanol. To a clear solution (0.01 mol) of purified succinic acid dihydrazide in 50 mL of ethanol, a mixture of 2-nitrobenzaldehyde (0.01 mol) and ferrocenecarboxaldehyde (0.01 mol) in 150 mL ethanol was added. After half an hour of stirring, the reaction mixture was refluxed for 6-7 hours. The progress of the reaction was checked at various time intervals using a thin-layer chromatographic technique. The cooled reaction mixture was filtered and the filtrate was concentrated to get reddish yellow colored *N*'1-((*E*)-2-(nitro)benzylidene)- *N*'4-((*E*)-2-(ferrocenylidene)succinohydrazide. Crude sample

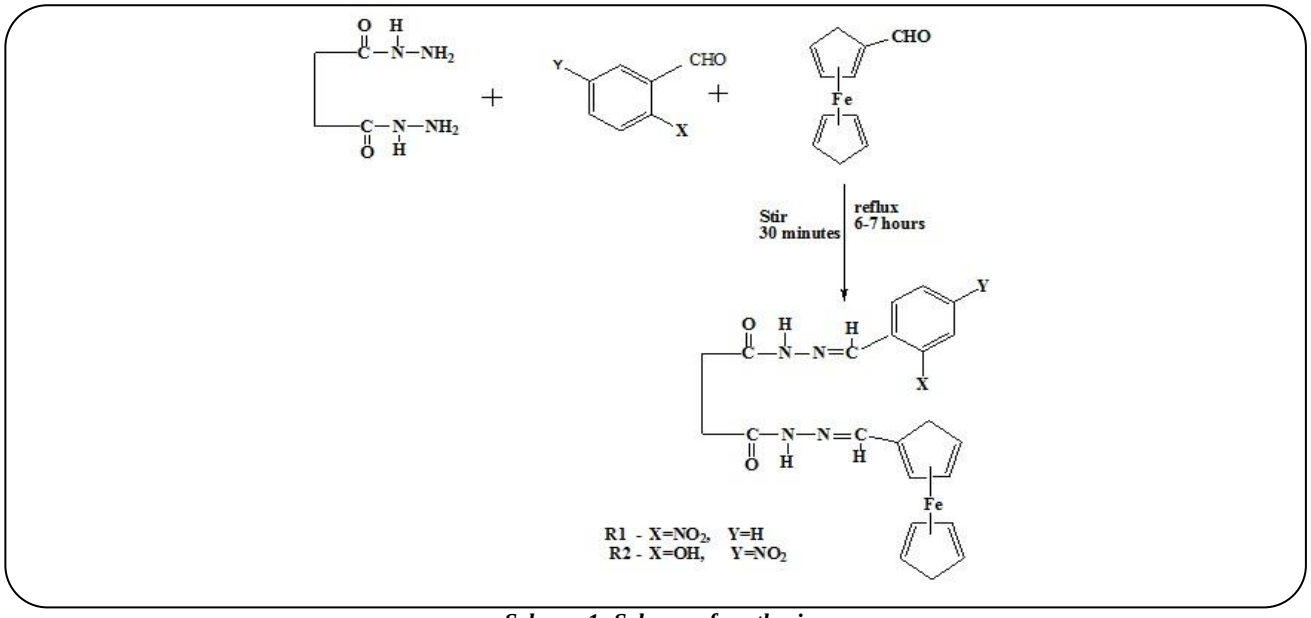

Scheme 1: Scheme of synthesis

was purified in a silica gel column using ethanol as eluent. Color: Dark reddish orange. Yield: 0.5332 g (91%), m.p. 180 °C.

Synthesis of N'1-((E)-2-hydroxy-5-(nitro)benzylidene)-N'4-((E)-2-(ferrocenylidene)succinohydrazide [R2]

Succinic acid dihydrazide solution (0.01 mole in 50 mL of ethanol) was added with stirring to another solution having 0.01 mole of 2-hydroxy-5- nitrobenzaldehyde and 0.01 mole of ferrocenecarboxaldehyde in 150 mL ethanol. The above mixture was stirred for half an hour and then refluxed for 6-7 hours. The thin-layer chromatographic technique was used to check the progress of the reaction at various time intervals. After cooling, the reaction mixture was filtered. The red colored solid was obtained after concentrating the filtrate. Purification of the crude product was carried out in a column having silica gel as the stationary phase and ethanol as eluent. Color: reddish orange, Yield: 0.6015 g, (91%), m.p. 182 ℃.

Binding energy calculation using molecular docking

Investigation of the binding manner of the manufactured compounds R1 and R2 with the target protein available in the microorganisms was done in Auto Dock version 1.5.6 [25] running on Windows 7. Target proteins of the enzymes were extracted from RCSB, Protein Data Bank (PDB). MGL tools of Auto Dock were employed to get the docking score. ChemSketch was engaged to draw the structures of the compounds R1 and R2 and converted them to 3D structures by utilizing 3D optimization tool. Ligands were geometrically optimized using a ligand module. Force field MMFF94 was engaged to compute the value of partial atomic charges. Selected proteins were docked with synthesized ligands using Auto Dock tools. H-bond interactions and binding affinity were analyzed for the best-docked pose obtained from conformation.

Assessment of antimicrobial activity

Experiments in triplicate were carried out using standard procedure [24] against two gram-positive bacteria, two gram-negative bacteria, and two fungi at appropriate temperatures. The average value arrived from the three experiments was considered for analysis.

Analysis of elements

Experimental data obtained on elemental analysis of the synthesized compounds match with the molecular formula values. R1 (Found (%): C, 55.65; H, 4.39; N, 14.70; Fe, 11.41; Calc. for $C_{22}H_{21}N_5O_4Fe$: C, 55. 60; H, 4.43; N, 14.76; Fe, 11.45). R2 (Found (%): C; 55.36; H, 4.10; N, 14.73; Fe, 11.40; Calc. for $C_{22}H_{21}N_5O_5Fe$: C, 55.30; H, 4.43; N, 14.76; Fe, 11.45). The presence of molecular peak (ESI) m/z at 474 and 482 respectively for the compounds *N*'1-((*E*)-2-(nitro)benzylidene)-*N*'4-((*E*)-2-(ferrocenylidene)succinohydrazide and *N*'1-((*E*)-2-hydroxy-5-(nitro)benzylidene)-*N*'4-((*E*)-2-(ferrocenylidene)

succinohydrazide on mass spectral analysis, confirm the formation of expected receptors.

FT-IR Spectral analysis

The FT-IR spectral peak of compound R1 observed around 487 cm^{-1} is related to the tilt stretching vibration of the ferrocene cyclopentadienyl ring and the 829 cm^{-1} peak corresponds to C-H out-of-plane bend vibration. The –C-C-H bending vibration in the cyclopentadienyl ring [26] emerged between 935 cm^{-1} to 1244 cm^{-1}. The peaks for symmetric stretching vibrations of $-NO_2$, -CH=N (imine) stretching vibration, and amide -C=O stretching arose at 1344 cm^{-1}, 1523 $cm^{-1,}$ and 1673 cm^{-1} respectively [27]. The stretching vibration of a secondary amine and water of hydration appeared as a single peak at 3199 cm^{-1}. The FT-IR spectral behavior of compound R2 is similar to that of R1 except for the intensity of 3199 cm^{-1} peak wherein the phenolic - OH group stretching vibration also merges with the stretching vibration of secondary amine and water of hydration.

NMR Spectral analysis

Nuclear magnetic resonance spectrum of R1 in C_2D_5OD solvent contains appropriate peaks and are assigned accordingly δ,(ppm); 8.4 (s, 2H, NCH), 7.5 (m, 4H, aromatic), 4.7 (m, 2H, cp subst), 4.2 (m, 2H, cp subst), 4.1 (s,5H, cp unsubst), 2.7 (2s, 4H, $2CH_2$), 1.2 (s, 2H, 2NH) (Fig. 1) for R2 δ, (ppm); 8.5 (s, 2H, NCH), 7-7.4 (m, 4H, aromatic), 4.5 (m, 2H, cp subst), 4.3 (m, 2H, cp subst), 4.1 (s,5H, cp unsubst), 2.7 (2s, 4H, $2CH_2$), 1.3 (s, 2H, 2NH).

RESULTS AND DISCUSSION

Examination of sensing behavior of R1 & R2

Compound R1 in acetonitrile exhibits two peaks around 249 nm & 281 nm and a broad peak near 469 nm (Fig. 2a). In alcohol, R1 displays two peaks near 251 nm and 289 nm (Fig. 2b). Aromatic ring π-π* transition is assigned for the peaks in the ultraviolet region [28] and d-d transition is earmarked for visible region peak [29].

UV-Visible titration method was engaged to find out the incarceration ability of receptors with various metal ions. About 2.5 mL of receptor solution (10^{-5} M) was taken in the quartz cell and 20 µL aliquots of metal solutions (10^{-2} M) were added. Absorbance spectra were recorded for metal ion-free and metal ion-added sensor solutions.

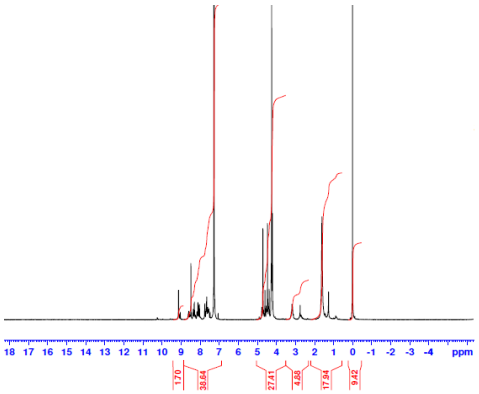

Fig.1: Proton NMR spectrum of sensor R1.

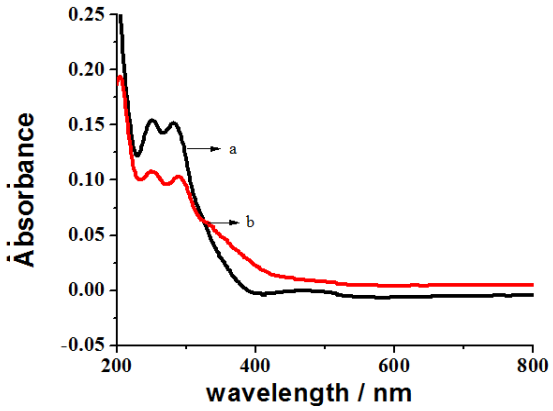

Fig. 2: Absorbance spectrum of R1 in a) acetonitrile b) ethanol.

Based on the solubility of selected metal salt for investigation, either the solution of receptor in acetonitrile or ethanol was utilized to chronicle the electronic spectra. Development of new peaks around 301 nm, 352 nm, and 457 nm for the addition of Cu^{2+} ions with the receptor at the expense of basic peaks of R1 exposes the sensing aptitude (Fig. 3a). The generation of 457 nm peak (Fig. 3b) which is responsible for the metal-to-ligand charge transfer [30] that has acquired after the coordination of Cu^{2+} ions with receptor also ascertains the sensing ability.

Successive addition of Hg^{2+}, $Ni^{2+,}$ and Pb^{2+} ions generate new peaks around 237, 246, and 238 nm respectively (Fig. 4) with simultaneous disappearance of peaks responsible for receptor. The cumulative addition of Mn^{2+} and Cd^{2+} ions resulted in an increase in absorbance value along all wavelength regions [28]. Above findings advocate that R1 is capable of sensing Cu^{2+}, Hg^{2+}, Pb^{2+}, Ni^{2+}, Mn^{2+} and Cd^{2+} ions.

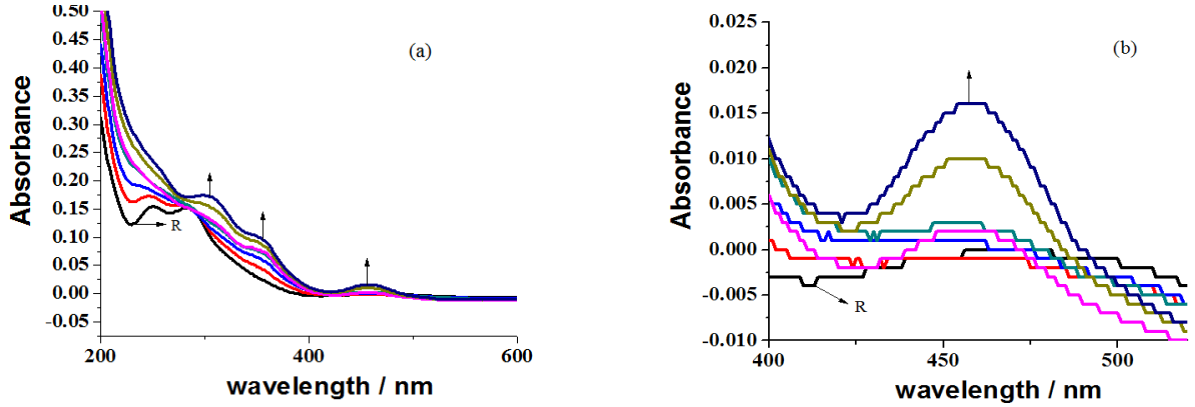

Fig. 3: a) Spectral changes noticed for the addition of Cu^{2+} ions to R1 b) Generation of MLCT band.

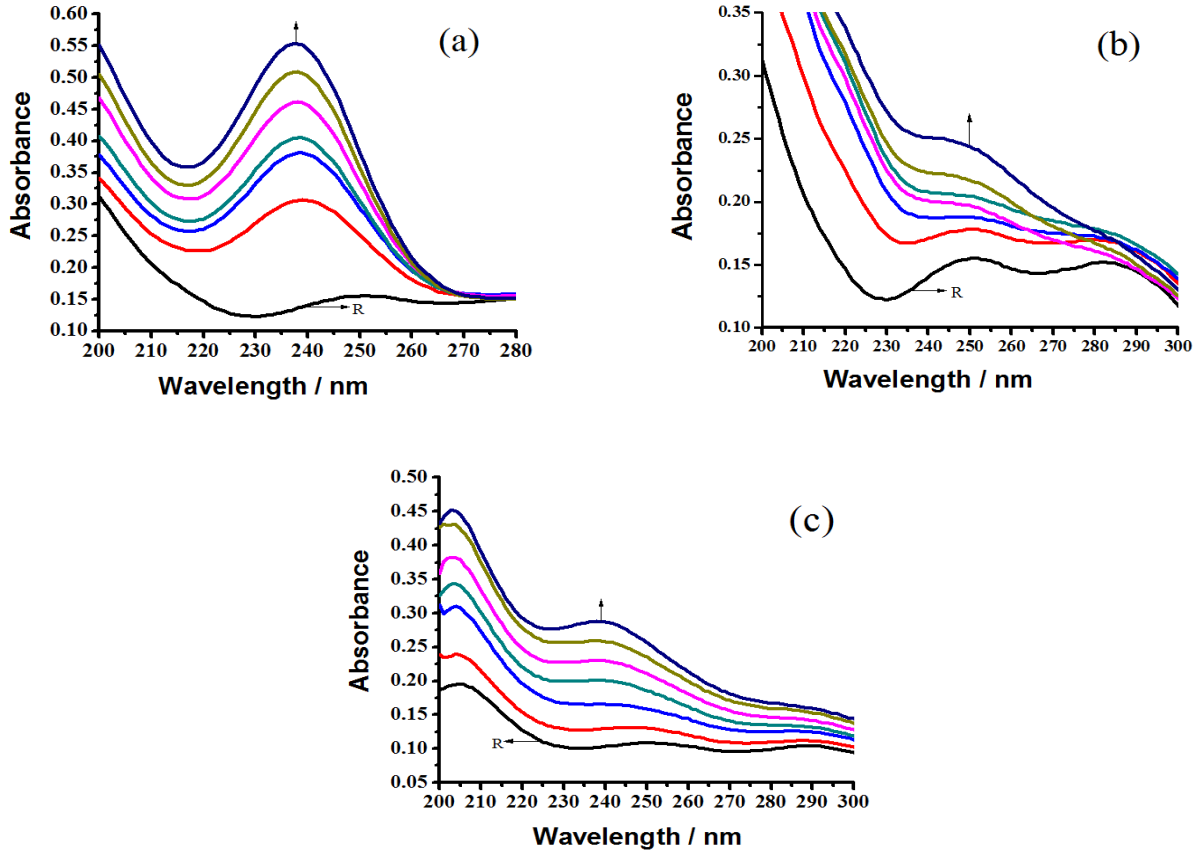

Fig.4: Development of a new peak in the spectrum of R1 for the addition of a) Hg^{2+}ions b) Ni^{2+} ions c) Pb^{2+} ions.

A shoulder around 282 nm in acetonitrile and a broad peak at 346 nm in ethanol solvents were recorded for the π- π* transition of compound R2. Formation of new peaks near 253 nm, 311 nm, and 461 nm (Fig. 5a, b, c) with the disappearance of 282 nm shoulder of the receptor for the successive addition of Cu^{2+} ions to R2 reveals the sensing ability of the receptor. Earlier report [30] had assigned metal-ligand charge transition for the appearance of a new peak around 460 nm.

The binding ability of R2 towards Hg^{2+}, $Mn^{2+,}$ and Cd^{2+} ions is exposed by the formation of a new peak at 240 nm for Hg^{2+} (Fig. 6a), conversion of broad peak to prominent peak around 346 nm for Mn^{2+} (Fig. 6b) and Cd^{2+} (Fig. 6c) respectively. The disappearance of the shoulder peak of

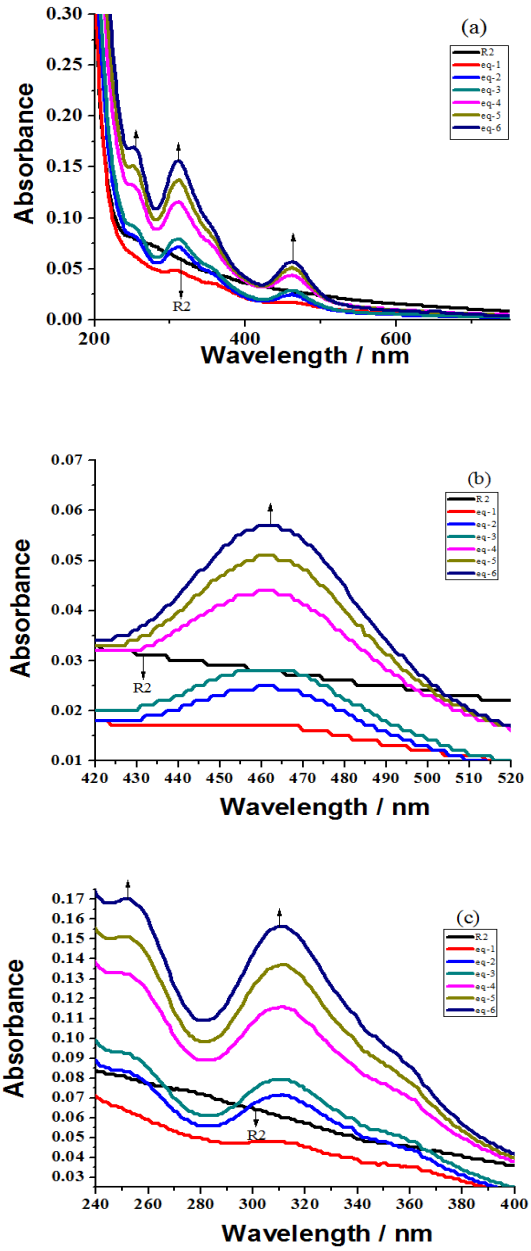

Fig.5: Spectral changes of R2 for the addition of Cu^{2}+ion a) Overall changes b) Generation of MLCT band c) Development of new peaks.

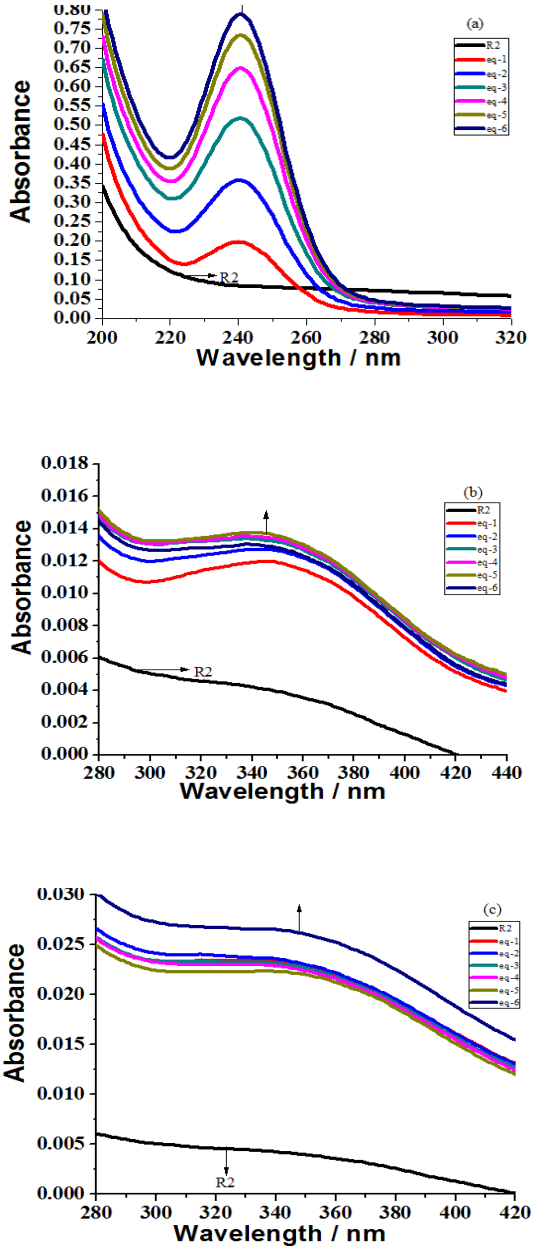

Fig.6: Appearance of a new peak in the spectrum of R2 for the addition of a) Hg^{2+} b) Mn^{2+} C) Cd^{2+}.

the receptor with increased absorbance value in all wavelength regions for the addition of Pb^{2+} and Ni^{2+} ions shows the sensing ability of R2 towards these metal ions.

Electrochemical investigation of sensing studies

Analysis of the voltammograms of R1 (Fig. 7) recorded with different scan rates for $1x10^{-3}$ M solution containing oxidation peak at 0.712 V and reduction peak around 0.566 V. Further increasing trend in ΔE_P, I_{pa} & I_{pc} values (Table 1) with an increase in scan rate is observed. Overblown ΔE_P values (146-161 mV, than the anticipated 59 mV) noticed for all scan rates suggest a quasi-reversible reduction of Fe^{2+} present in ferrocene moiety [31].

CV- titration studies were carried out by adding 20 µL (using micropipette) of either $1x10^{-3}$ M (Fig. 8a) or $1x10^{-1}$ M (Fig. 8b) metal salts solution to 10 mL of $1x10^{-3}$ M R1

Table 1: Electrochemical parameters for R1.

Scan Rate- mV/ sec	E_{pa} (V)	E_{pc} (V)	ΔE_p (V)	$E_{1/2}$ (V)	I_{pa} x10^{-6} (µA)	I_{pc} x10^{-6} (µA)
Solvent -Acetonitrile						
20	0.712	0.566	0.146	0.639	-2.907	1.779
50	0.721	0.566	0.155	0.643	-4.590	3.260
100	0.719	0.564	0.155	0.641	-6.411	4.978
Solvent - Ethanol						
20	0.712	0.551	0.161	0.631	-2.564	1.311
50	0.708	0.559	0.149	0.633	-3.811	2.625
100	0.706	0.555	0.151	0.630	-5.327	4.245

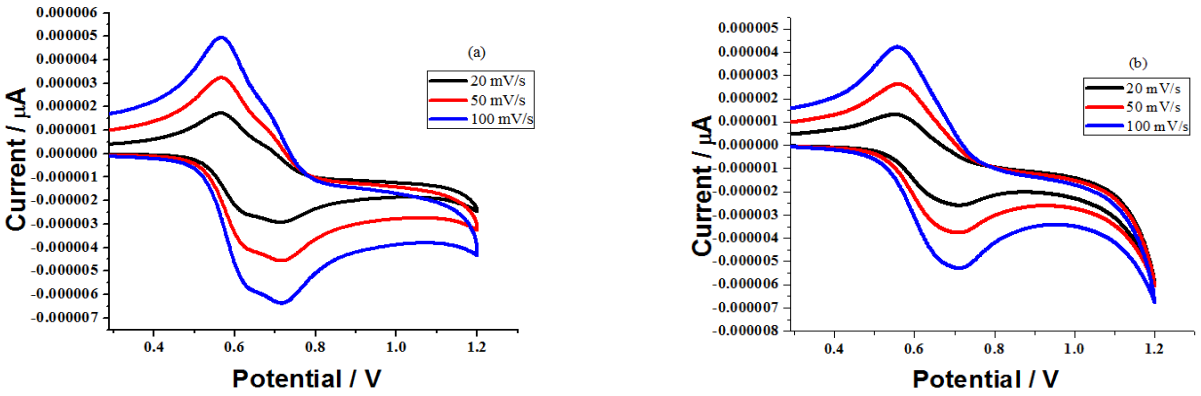

Fig.7: Cyclic voltammogram of R1 recorded with different scan rate a) acetonitrile b) ethanol.

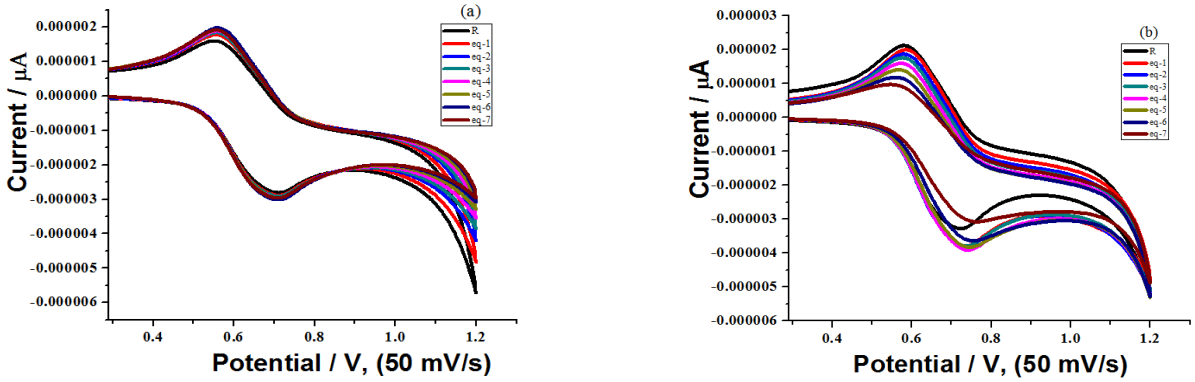

Fig.8: Changes in voltammogram of R1 for the addition of Cd^{2+} ions a) 1x10^{-3} M b) 1x10^{-1} M.

a solution taken in the three-compartment cell up to 7 equivalents and cyclic voltammograms (scan rate - 50 mV/s) were recorded for each addition. Changes in voltammograms contain positive potential shifts for the oxidation peak and negative potential shifts for the reduction peak which support the interaction operating between the receptor and added metal ions [32]. As an example, the voltammograms registered for the addition of Cd^{2+} ions are presented in Fig. 8.

A varied amount of I_{pa} values observed (Table 2) for the addition of dissimilar metal ions (Fig. 9) having 1x10^{-3} M concentration exposes the difference in binding aptitude of

Table 2: Electrochemical data for the addition of various metal ion solution (R1, 10^{-3} M / M^{2+}, 10^{-3} M) (Scan Rate - 50 mV/s).

Addition	E_{pa} (V)	E_{pc} (V)	ΔE_p (V)	$E_{1/2}$ (V)	I_{pa} x10^{-6} (µA)	I_{pc} x10^{-6} (µA)
Solvent - Acetonitrile						
Receptor	0.721	0.566	0.155	0.643	-4.590	3.260
Cu^{2+}	0.719	0.566	0.153	0.637	-4.652	3.314
Ni^{2+}	0.721	0.564	0.157	0.642	-5.553	3.704
Hg^{2+}	0.706	0.558	0.148	0.632	-5.434	4.032
Solvent - Ethanol						
Receptor	0.708	0.559	0.149	0.633	-3.811	2.625
Cd^{2+}	0.710	0.553	0.157	0.631	-2.898	1.769
Mn^{2+}	0.708	0.559	0.149	0.633	-3.846	2.743
Pb^{2+}	0.702	0.559	0.143	0.630	-3.846	2.620

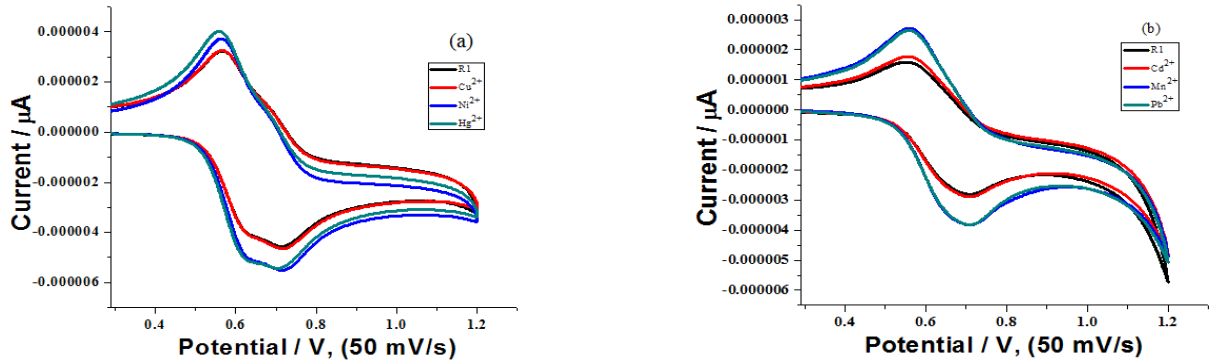

Fig. 9: Cyclic voltammograms recorded (scan rate - 50 mV/s) for the addition of different metal ion to R1 a) acetonitrile b) ethanol.

metal cations. Apart from that, it is a measure of repulsive force existing between the oxidized ferrocene moiety and coordinated metal cation [33]. The percentage difference in I_{pa} values (ΔI_{pa} %) calculated for the oxidation current value of receptor solution and metal ions added to receptor solution reflects the sensing order of R1 as Cd (32.6) > Hg (20.8) > Ni (11.9) > Mn (4.3) > Cu (1.6) > Pb (1.9).

The ΔI_{pa} (%) values (Table 3) calculated from the noted I_{pa} values for the addition of 1x 10^{-1} M metal salt solutions to 1x 10^{-3} M R1 solution disclose the sensing power of R1 as Cd^{2+} (24.3) > Mn^{2+} (9.7) > Ni^{2+} (9.1) > Cu^{2+} (8.4) > Pb^{2+} (7.6) > Hg^{2+} (3.8). Careful analysis of the ΔI_{pa} (%) values estimated for the addition of 1x10^{-3} M and 1x10^{-1} M concentrations of various metal ions convey that R1 is potent towards Cd, Hg & Ni at lower concentrations and persuasive to Cd, Mn & Ni at higher concentration (Fig. 10).

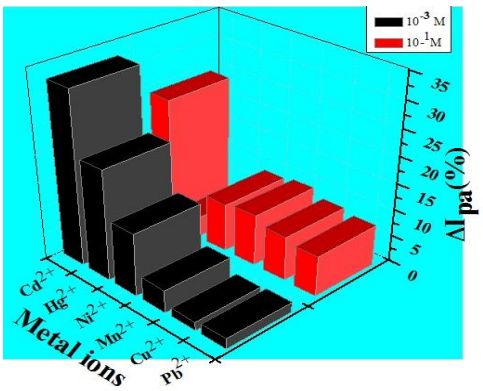

Fig.10: Comparison chart for sensing ability of R1.

The inclination of voltammograms perceived for R2 with different scan rates is similar to R1 with an increase in value of ΔE_P, $I_{pa,}$ and I_{pc} (Table 4).

Table 3: CV data obtained (scan rate- 50 mV/s) for the addition of 1x10^{-1}M metal salt solutions to 1x10^{-3} M R1.

Addition	E_{pa} (V)	E_{pc} (V)	ΔE_p (V)	$E_{1/2}$ (V)	I_{pa} x10^{-6} (µA)	I_{pc} x10^{-6} (µA)
Solvent - Acetonitrile						
Receptor	0.721	0.566	0.155	0.643	-4.590	3.260
Cu^{2+}	0.723	0.595	0.128	0.659	-4.684	2.983
Ni^{2+}	0.725	0.595	0.13	0.66	-5.821	3.585
Hg^{2+}	0.739	0.603	0.136	0.671	-4.413	3.134
Solvent - Ethanol						
Receptor	0.708	0.559	0.149	0.633	-3.811	2.625
Cd^{2+}	0.729	0.584	0.145	0.656	-3.806	1.987
Mn^{2+}	0.715	0.582	0.407	0.648	-3.338	2.370
Pb^{2+}	0.719	0.586	0.133	0.652	-3.477	2.425

Table 4: Electrochemical parameters for R2 with different scan rate.

Scan Rate mV/s	E_{pa} (V)	E_{pc} (V)	ΔE_p (V)	$E_{1/2}$ (V)	I_{pa} x10^{-6} (µA)	I_{pc} x10^{-6} (µA)
Solvent -Acetonitrile						
20	0.725	0.576	0.149	0.650	-1.227	0.531
50	0.727	0.576	0.151	0.648	-1.969	1.079
100	0.723	0.581	0.142	0.652	-2.846	1.806
Solvent - Ethanol						
20	0.694	0.607	0.087	0.650	-1.779	-1.853
50	0.694	0.593	0.101	0.643	-2.096	3.530
100	0.701	0.593	0.108	0.647	-2.745	1.118

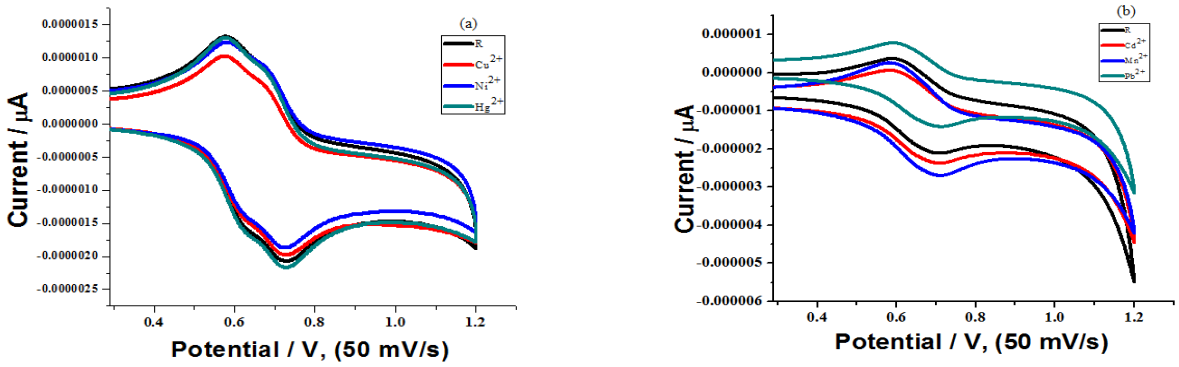

Fig.11: Voltammograms (scan rate- 50 mV/s) recorded for the addition of different metal ions to R2 a) acetonitrile b) ethanol.

Employing the same procedure utilized for R1, CV titration studies (scan rate - 50 mV/s) were carried out for R2 with various metal salts solutions (Fig.11) and the difference in I_{pa} amount noticed (Table 5) exposes the change in the ability of the receptor to bind with the different metal ion. Binding order priority based on the ΔI_{pa} (%) under equimolar addition (Table 5) is Pb^{2+} (54.9%) > Cd^{2+} (33.1%) > Mn^{2+} (21.5%) > Hg^{2+} (17.5) > Ni^{2+} (12.3) > Cu^{2+} (4.7)

Table 5: CV titration data (scan rate- 50 mV/s) for the addition of 1x10^{-3} M metal salt solution to 1x10^{-3} M R2.

Addition	E_{pa} (V)	E_{pc} (V)	ΔE_p (V)	$E_{1/2}$ (V)	I_{pa} x10^{-6} (µA)	I_{pc} x10^{-6} (µA)
Solvent - Acetonitrile						
Receptor	0.727	0.576	0.151	0.648	-1.969	1.079
Cu^{2+}	0.729	0.574	0.155	0.651	-1.993	1.028
Ni^{2+}	0.723	0.580	0.143	0.651	-1.859	1.230
Hg^{2+}	0.727	0.578	0.149	0.652	-2.185	1.309
Solvent - Ethanol						
Receptor	0.694	0.593	0.101	0.643	-2.096	3.530
Cd^{2+}	0.704	0.586	0.121	0.645	-2.362	5.278
Mn^{2+}	0.702	0.586	0.116	0.644	-2.718	2.771
Pb^{2+}	0.704	0.595	0.109	0.649	-1.425	7.829

Table 6: CV titration data (scan rate- 50 mV/s) for the addition of 1x10^{-3} M metal salt solution to 1x10^{-1} M R2.

Addition	E_{pa} (V)	E_{pc} (V)	ΔE_p (V)	$E_{1/2}$ (V)	I_{pa} x10^{-6} (µA)	I_{pc} x10^{-6} (µA)
Solvent - Acetonitrile						
Receptor	0.727	0.576	0.151	0.648	-1.969	1.079
Cu^{2+}	0.715	0.599	0.116	0.657	-2.978	1.830
Ni^{2+}	0.772	0.634	0.138	0.703	-2.390	1.341
Hg^{2+}	0.783	0.640	0.143	0.711	-1.901	1.270
Solvent - Ethanol						
Receptor	0.694	0.593	0.101	0.643	-2.096	3.530
Cd^{2+}	0.762	0.659	0.103	0.710	-1.469	5.483
Mn^{2+}	0.696	0.605	0.091	0.650	-1.235	6.451
Pb^{2+}	0.770	0.663	0.107	0.716	-1.661	9.064

and multimolar addition (Table 6) is Pb^{2+} (61) > Mn^{2+} (45) > Cu^{2+} (41) > Cd^{2+} (35%) > Hg^{2+} (15) > Ni^{2+} (14.3). Fig. 12 symbolizes the comparison between the sensing ability of R2 and the moderate metal concentration of metal ions required.

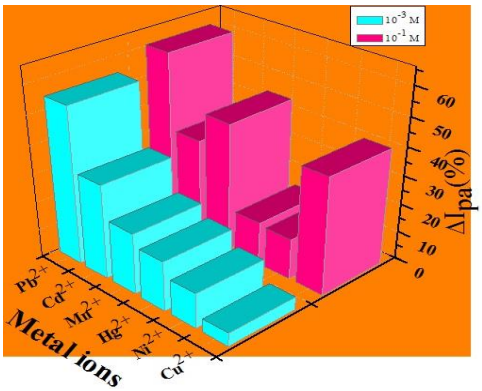

Fig. 12: Comparison chart for sensing ability of R2.

Antimicrobial Studies

Antibacterial activity of R1 & R2 was carried out by disc diffusion method, having Mueller Hinton Agar base, against *Streptococcus faecalise*, *Staphylococcuse aureuse*, *Salmonella typhimurium* and *Escherichia coli* (Fig. 13) and anti-fungal studies were conducted with Sabouraud's Dextrose agar as a base against fungi *Candida albicans*

Table 7: In-vitro antimicrobial studies data.

S.No	Microorganisms	Control	R1	R2	Ciprofloxacin/Ketoconazole
zone of inhibition in mm for bacteria					
1	Staphylococcus aureus	-	12	06	25
2	Streptococcus faecalis	-	-	-	24
3	Escherichia coli	-	09	07	12
4	salmonella typhimurium	-	10	08	27
zone of inhibition in mm for fungi					
1	Candida albicans	-	-	06	06
2	Aspergillus niger	-	12	10	25

Fig. 13: Zones of inhibition for a) SA b) SF c) ST d) EC.

Fig.14: Zones of inhibition for a) CA b) AN.

and *Aspergillus niger* (Fig. 14). Data of growth inhibition distance perceived for R1 & R2 in the antimicrobial analysis are presented in Table 7.

Compound R2 prohibition efficiency against fungi *Candida albicans* is 100% in comparison with the standard drug ketoconazole, which is unusual and demands more focused research by the pharmacist to develop a new formulation of antifungal agent [22]. The resistivity of R1 and R2 to resist the growth of fungi *aspergillus niger* is also comes to around 50%. The retardant nature of R1 & R2 towards bacteria is on par with standard ciprofloxacine, except for *Streptococcus faecalis*.

Molecular docking studies

Molecular docking studies were carried out using software, mentioned in the experimental section, for the proteins of the microorganisms as stated here: 6TZ6- *Candida albicans*, 3K4Q- *Aspergillus niger*, 7BU2- *Escherichia coli*, 4YXB- *salmonella typhimurium*, 6KVQ -*Staphylococcus aureus* and 1PTF- *Streptococcus faecalis* and the results arrived are presented in (Table 8) The binding posture of the ligand and proteins in 3D and 2D angle are given in figure –15. Fungi proteins 3K4Q & 6TZ6 bind comfortably with both the ligands by giving binding energy value greater than -5 Kcal mol^{-1} which exposes the higher antifungal activity of newly synthesized receptors [34]. In addition to that compound R1 & R2 displayed better scores against bacteria proteins 4YXB & 7BU2.

CONCLUSIONS

Unsymmetrical Schiff base compounds comprising of ferrocene occupied azomethine group at one side and aromatic aldehyde attached mine on the other side is prepared in a single step reaction. The newly synthesized materials *N*'1-((*E*)-2-(nitro)benzylidene)-*N*'4-((*E*)-2(ferrocenylidene)succinohydrazide and *N*'1-((*E*)-2-hydroxy-5-(nitro)benzylidene)-*N*'4-((*E*)-2-(ferrocenylidene)succinohydrazide were upheld by FT-IR, ^{1}HNMR and Mass spectrum analysis. Ability of the

Table 8: Data obtained in molecular docking studies.

PDB	Free binding energy, kcal mol^{-1}		R1		R2	
	R1	R2	Formation of hydrogen bonds with receptor and amino acids	Distance(Å)	Formation of hydrogen bonds with receptor and amino acids	Distance(Å)
1PTF	-4.04	-3.09	33-ILE 45-LYS 43-ASN	3.24 3.18 3.39	82-GLN 78-VAL	3.64 3.38
3K4Q	-5.16	-5.79	49-ARG 123-ARG 124-TYR	3.18 3.28 3.31	271-ASP 272-TYR 366-ILE	3.21 3.86 3.96
4YXB	-4.55	-7.57	25-PHE 27-ASP 45-PRO	3.54 3.17 3.27	25-PHE 27-ASP 47-GLU	3.42 3.27 3.12
6KVQ	-3.14	-3.98	116-VAL 115-PRO 119-LYS	2.98 3.38 3.62	25-ASN 139-GLU 179-MET 183-ALA	3.85 3.28 3.31 3.96
6TZ6	-6.29	-6.33	58-GLN 97-TYR	3.40 3.82	40-PHE 46-ARG 59-VAL 97-TYR	2.78 3.86 3.75 3.85
7BU2	-5.42	-7.81	264-VAL 284-GLY	3.96 3.47	261-VAL 263-ALA 332-ARG	3.47 3.76 3.18

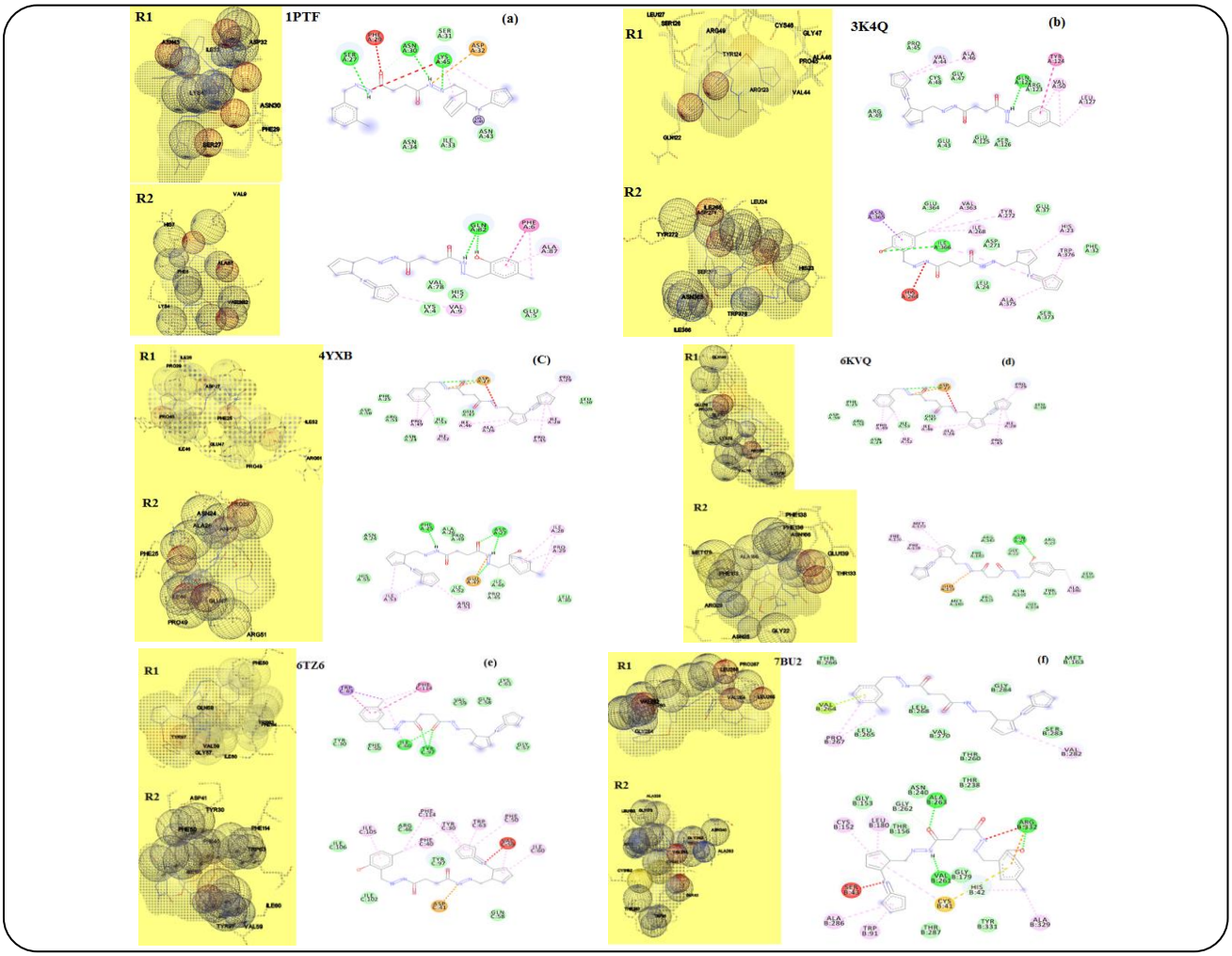

Fig.15: 3D and 2D view binding of R1 and R2 with a) 1PTF b) 3K4Q c) 4YXB d) 6KVQ e) 6TZ6 f) 7BU2.

receptor to sense Hg^{2+}, Pb^{2+}, Cd^{2+}, Mn^{2+}, Ni^{2+} and Cu^{2+} ions is identified in UV-Visible titration method. The effective concentration of metal ions required for a particular concentration of sensor solution is arrived at from the percentage amount of ΔI_{pa} values calculated from the anodic current values (I_{pa}) noticed from the cyclic voltammograms recorded for the receptor solution containing different metal ions. Hundred percent efficiency, to prevent the growth of the fungus *Candida albicans* by compound R2, is recognized from *in-vitro* and molecular docking studies which entice pharmaceutical research to be undertaken.

Acknowledgment

The authors acknowledge the support from *Dr. K. Pandian*, Professor of Inorganic Chemistry & Controller of Examinations, University of Madras for the UV-Visible spectral studies free of cost. The help extended by *Dr. K. Ilango*, Professor, Department of Pharmaceutical Chemistry, SRM College of Pharmacy, SRM Institute of Science and Technology, Kattankulathur-603 203, Chengalpattu District, Tamil Nadu, India, in analyzing the molecular docking results is gratefully acknowledged by the authors. The research scholar D.Saranya wishes to record her thanks to the State Government of Tamil Nadu, India for the annual research assistant grant.

Received : Jul. 30, 2021 ; Accepted : Nov. 8, 2021

REFERENCES

[1] Sanjoy Singh T., Paul P.C., Harun Pramanik A.R., Fluorescent Chemosensor Based on Sensitive Schiff Base for Selective Detection of Zn^{2+}, *Spectrochimica Acta Part A: Molecular and Biomolecular Spectroscopy*, **121**: 520–526(2014).

[2] Gale P.A., Caltagirone C., Anion Sensing by Small Molecules and Molecular Ensembles, *Chemical Society Reviews*, **44**: 4212–4227(2015).

[3] Bagher-Gholivand M., Babakhanian A., Mohammadi M., Moradi P., Kiaie S.H., Novel Opticalbulk Membrane Sensor and its Application for Determination of Iron in Plant and Cereal Samples, *Journal of Food Composition and Analysis*, **29(2)**: 144–150 (2013).

[4] Rostami-Javanroudi S., Babakhanian A., New Electrochemical Sensor for Direct Quantification of Vitamin K in Human Blood Serum, *Microchemical Journal*, **163**: 105716(2021).

[5] Babakhanian A., Momeneh T., Aberoomand-azar P., Kaki S., Torki M., Hossein Kiaie S., Dabirian F., A Fabricated Electro-Spun Sensor Based on Lake Red C pigments Doped into PAN (polyacrylonitrile) Nano-Fibers for Electrochemical Detection of Aflatoxin B1 in Poultry Feed and Serum Samples, *The Analyst*, **140(22)**: 7761–7767 (2015).

[6] Bansod B., Kumar T., Thakur R., Rana S., Singh I., A Review on Various Electrochemical Techniques for Heavy Metal Ions Detection with Different Sensing Platforms, *Biosensor and Bioelectronics*, **94**: 443-455 (2017).

[7] Gong T., Liu J., Liu X., Liu J., Xiang J., Wu Y., A Sensitive and Selective Sensing Platform Based on CdTe QDs in the Presence of L-Cysteine for Detection of Silver, Mercury and Copper Ions in Water and Various Drinks, *Food Chemistry*, **231**: 306-3129 (2016).

[8] Abu-Dief AM., Mohamed IM., A Review on Versatile Applications of Transition Metal Complexes Incorporating Schiff Bases, *Journal of Basic and Applied Sciences*, **4**: 119–133 (2015).

[9] Babakhanian A., Gholivand M.B., Mohammadi M., Khodadadian M., Shockravi A., Abbaszadeh M., Ghanbary A., Fabrication of a Novel Iron(III)–PVC Membrane Sensor Based on a New 1,1′-(iminobis(methan-1-yl-1-ylidene))dinaphthalen-2-ol Synthetic Ionophore for Direct and Indirect Determination of Free Iron Species in Some Biological and Non-Biological Samples, *Journal of Hazardous Materials*, **177(1-3)**: 159–166(2010).

[10] Babakhanian A., Momeneh T., Aberoomand-azar P., Kaki S., Torki M., Hossein Kiaie S., Dabirian F., A Fabricated Electro-Spun Sensor Based on Lake Red C Pigments Doped into PAN (polyacrylonitrile) Nano-Fibers for Electrochemical Detection of Aflatoxin B1 in Poultry Feed and Serum Samples, *The Analyst*, **140(22)**: 7761–7767(2015).

[11] Su Q., Niu Q., Sun T., Li T., A Simple Fluorescence Turn-on Chemosensor Based on Schiff-Base for Hg^{2+}-Selective Detection, *Tetrahedron Letters*, **57:** 4297–4301(2016).

[12] Forsberg Z., Stepnov A.A., Kruge Nærdal G., Klinkenberg G., Chapter One–Engineeringlytic Polysaccharide Monooxygenases (LPMOs), *Methods in Enzymology*, **644**:1-34 (2020).

[13] Bao J., Xing Y., Feng C., Kou S., Jiang H., Li X., Acute and Sub-Chronic Effects of Copper on Survival, Respiratory Metabolism, and Metal Accumulation in Cambaroides Dauricus, *Scientific Reports*, 1-9 (2020)

[14] Barber R.G., Grenier Z.A., Burkhead J.L., Copper Toxicity Is Not Just Oxidative Damage: Zinc Systems and Insight from Wilson Disease, *Biomedicines*, **9**: 316 (2021).

[15] Chen H., Giri N.C., Zhang R., Yamane K., Zhang Y. Maroney M., Costa M., Nickel Ions Inhibit Histone Demethylase JMJD1A and DNA Repair Enzyme ABH2 by Replacing the Ferrous Iron in the Catalytic Centers, *Journal of Biological Chemistry*, **292**: 10743-10743 (2017).

[16] Tarnacka B., Jopowicz A., Maślińska M., Copper, Iron, and Manganese Toxicity in Neuropsychiatric Conditions, *International Journal of Molecular Sciences*, **22(15)**: 7820 (2021)**.**

[17] Branca J.J.V., Pacini A., Gulisano M., Taddei N., Fiorillo C., Becatti M., Cadmium-Induced Cytotoxicity: Effects on Mitochondrial Electron Transport Chain, *Frontiers in Cell and Developmental Biology*, **8:** 1-7(2020).

[18] Kumar A., Kumar A., Cabral-Pinto M.M.S., Chaturvedi A.K., Shabnam A.A., Subrahmanyam G., Mondal R., Kumar Gupta D., Malyan S.K.., Kumar S.S., Khan S.A., Yadav K.K., Lead Toxicity: Health Hazards, Influence on Food Chain, and Sustainable Remediation Approaches, *International Journal of Environmental Research Public Health*, **17**: 2179 (2020).

[19] Mahmoud W.H., Deghadi R.G., Mohamed G.G., Novel Schiff Base Ligand and its Metal Complexes with Some Transition Elements. Synthesis, Spectroscopic, Thermal Analysis, Antimicrobial and in Vitro Anticancer Activity, *Applied Organometallic Chemistry*, **30**: 221- 230 (2016).

[20] Nasir Uddin M., Samina Ahmed A., Rahatul Alam S.M., Biomedical Applications of Schiff Base Metal Complexes, *Journal of Coordination Chemistry*, **73(23)**: 3109-3149(2020).

[21] Suzan A., Matar Wamidh H., Talib Mohammad S., Mustafa Mohammad S., Mubarak Murad Al Damen A.., Synthesis, Characterization, and Antimicrobial Activity of Schiff Bases Derived from Benzaldehydes and 3,30-diaminodipropylamine, *Arabian Journal of Chemistry*, **8**: 850-857(2015).

[22] Buda De Cesare G., Cristy S.A., Garsin D.A., Lorenz M.C., Antimicrobial Peptides: A New Frontier in Antifungal Therapy, *mBio*., **11**: e02123-20(2020).

[23] Farouk Kandil., Mohamad Khaled Chebani., Wail Al Zoubi., Synthesis of Macrocyclic Bis-Hydrazone and Their Use in Metal Cations Extraction, *ISRN Organic Chemistry*, **8**: 208284 (2012).

[24] Bagamboula C.F, Uyttendaele., Debevere J., Inhibitory Effect of Thyme and Basil Essential Oils, Carvacrol, Thymol, Estragol, Linalool and P-Cymene Towards Shigella Sonnei and S. Flexneri, *Food Microbiology*, **21**: 33 (2004).

[25] Morris G.M., Huey R., Lindstrom W., Sanner M. F., Belew R.K., Goodsell D.S., Olson A.J., AutoDock4 and AutoDockTools4: Automated Docking with Selective Receptor Flexibility, *Journal of Computational Chemistry*, **30**: 2785 (2009).

[26] Erkhova L.V., Presniakov I.A., Afanasov M.I., Lemenovskiy D.A., Yu H., Wang L., Danilson M., Koel M., Ferrocene Introduced into 5-Methylresorcinol-Based Organic Aerogels, *Polymers*, **12**: 1582 (2020).

[27] Mandewale M.C., Thorat B., Nivid Y., Nagarsekara R.A.J., Yamgar R., Synthesis, Structural Studies and Antituberculosis Evaluation of New Hydrazone Derivatives of Quinolone and their Zn(II) Complexes, *Journal Saudi Chemical Society*, **22:** 218 (2016).

[28] Benramdane R., Benghanem F., Ourari A., Keraghel S., Bouet G., Synthesis and Characterization of a New Schiff Base Derived from 2,3-diaminopyridine and 5 methoxysalicylaldehyde and its Ni(II), Cu(II) and Zn(II) Complexes. Electrochemical and Electrocatalytical Studies, *Journal of Coordinational Chemistry*, **68**: 560 (2015).

[29] Cheng J., Ma X., Zhang Y., Liu J., Zhou X., Xiang H., Optical Chemosensors Based on Transmetalation of Salen-Based Schiff Base Complexes, *Inorganic Chemistry*, **53**: 3210−3219 (2014).

[30] Lüthi E., Forero Cortés P.A., Prescimone A., Constable E.C., Housecroft C.E., Schiff Base Ancillary Ligands in Bis(diimine) Copper(I) Dye-Sensitized Solar Cells, *International Journal of Molecular Sciences*, **21(5)**: 1735 (2020).

[31] Kamatchi P., Selvaraj S., Kandaswamy M., Synthesis, Magnetic and Electrochemical Studies of Binuclear Copper(II) Complexes Derived from Unsymmetrical Polydentate Ligands, *Polyhendron*, **24**: 900(2005).

[32] Mondal A., Chowdhury A.R., Bhuyan S., Mukhopadhyaye S.K., Banerjee P., A Simple Urea-Based Multianalyte and Multichannel Chemosensor for the Selective Detection of F−, Hg^{2+} and Cu^{2+} in Solution and Cells and the Extraction of Hg^{2+} and Cu^{2+} from Real Water Sources: A Logic Gate Mimic Ensemble, *Dalton Transactions*, (2019).

[33] Kamal A., Kumar S., Kumar V., Mahajan R.K., Selective Sensing Ability of Ferrocene Appended Quinoline-Triazolederivative Toward Fe (III) Ions, *Sensors and Actuators B: Chemical*, **22**: 370 (2015).

[34] Khashi M., Beyramabadi S.A, Gharib A., Novel Schiff Bases of Pyrrole: Synthesis, Experimental and Theoretical Characterizations, Fluorescent Properties and Molecular Docking, *Iran. J. Chem. Chem. Eng. (IJCCE)*, **37(6)**: 59-72 (2018).